Excitation functions of the proton-induced nuclear reactions on titanium

Sinthia Binte Kholil[1,2], M. Shuza Uddin[1,*] Ingo Spahn[3], M. Mehedi Hasan[1], A. Kumer Chakroborty[2], M. Asad Shariff[1], M. Shamsuzzoha Basunia[4], Syed M. Qaim[3]

[1] *Tandem Accelerator Facilities, INST, Atomic Energy Research Establishment, Savar, Dhaka, Bangladesh*
[2] *Department of Physics, Chittagong University of Engineering and Technology, Chittagong, Bangladesh*
[3] *Institut für Neurowissenschaften und Medizin, INM-5: Nuklearchemie, Forschungszentrum Jülich, D-52425 Jülich, Germany*
[4] *Nuclear Science Division, Lawrence Berkeley National Laboratory, Berkeley, California 94720, USA*

Abstract

Excitation functions of proton-induced nuclear reactions on natural titanium were measured using stacked target activation from reaction thresholds up to 44.28 MeV. A wide energy range was achieved by irradiating several stacks with proton beams of energies 16.7 MeV, 27 MeV, and 44.5 MeV. Cross-section data were obtained from 15 to 25 MeV at the Lawrence Berkeley National Laboratory (LBNL) and from 14 to 44.28 MeV and 8 to 17 MeV at Forschungszentrum Jülich (FZJ). Each set of measured data agrees well with each other in the overlapping energy regions. The cross sections were also calculated theoretically using the TALYS code, and the model calculations reproduced the experimental values well. Generally, the results obtained for proton-induced reactions using the global set of parameters, as expressed in the TENDL-2021 data library, are not satisfactory. Our measurements are valuable for resolving discrepancies in the existing data, optimizing medical isotope production, and providing insights into reaction mechanisms.

1. Introduction

Medium-energy proton-induced nuclear reactions on titanium are of considerable significance in nuclear research: both fundamental investigations and application-oriented studies. It is an important element in nuclear technology and is as a target material in accelerator production of medical radioisotopes, namely ^{44}Sc, ^{47}Sc, etc. The natural composition consists of five stable isotopes, namely ^{46}Ti (8.25%), ^{47}Ti (7.44%), ^{48}Ti (73.72%), ^{49}Ti (5.41%) and ^{50}Ti (5.18%). The theranostic approach entails a combination of diagnosis (molecular imaging) and internal

* Author for correspondence, E-mail: md.shuzauddin@yahoo.com

radionuclide therapy (molecular targeted treatment). It makes use of two radionuclides of the same element in the same chemical form, a positron emitter which allows quantitative diagnosis and a therapeutic nuclide. This methodology is occasionally termed as personalized medicine. Originally, the pair $^{44g}Sc/^{47}Sc$ was developed [cf. 1], the radionuclide ^{44g}Sc is an interesting positron emitter ($T_{1/2}$ = 3.93 h; Eγ= 511keV, Iγ= 188.68%; $E_{\beta+}$=1475.3keV, $E_{\beta+}$= 94.34%) where ^{47}Sc ($T_{1/2}$= 3.35 d) emits a β^- particle as well as a low-energy γ-ray, which could be utilized for SPECT measurement to deliver data for dosimetry. However, in this case the dosimetry is not quantitative.

The cross sections of the $^{nat}Ti(p,x)^{48}V$ and $^{nat}Ti(p,x)^{46}Sc$ reactions are well established and currently used as beam monitors. Using several monitor reactions induced in a single foil is a good option for checking the incident particle energy via the activity ratio of the radionuclides [2]. Therefore, additional measurements and intercomparisons are necessary for a meaningful evaluation. The present status of data for other radionuclides produced via proton-induced activation on titanium is rather weak. Several groups have reported data over various proton energy ranges (Ep= 45→3 MeV) [cf. 3–14]; however, a arge discrepancies have been found among them. In most cases, a primary proton energy of around 45 MeV was used, expanded to the lowest energy of 3 MeV via the stacked targets technique, which introduces significant uncertainty in proton energy in the lower energy region. This is one of the reasons for the discrepancies. To resolve these discrepancies, this study undertakes detailed experimental measurements using proton beams with primary energies of 16.7, 27, and 44.5 MeV. Consequently, three data sets from reaction thresholds to 44.28 MeV were obtained.

The model calculations were performed using TALYS-1.95 code and compared with our measured values. However, using global parameters from the TENDL file often results in unsatisfactory predictions. Therefore, we focused on selecting specific input parameters to better match the experimental results.

2 Experimental

2.1 Sample preparation and irradiations

Excitation functions of the proton-induced reactions on natural titanium were measured by the stacked-sample activation technique. The 25 μm thick Ti foils of natural isotopic composition (supplied by Good Fellow; purity: >99.6 %) were cut in circular discs with a diameter of 13 mm. These foils were also used as beam monitors. Six ^{nat}Ti-containing stacks were irradiated with protons. One irradiation with 27±0.3 MeV primary energy protons was carried out for 30 min at a beam current of 100 nA at the 88-inch cyclotron, Lawrence Berkeley National Laboratory (LBNL), USA. Three stacks were irradiated individually for 30 min with 16.7±0.2 MeV primary energy protons using the BC 1710 cyclotron at FZJ, Germany, and the beam current was kept constant at about 200 nA. Other two stacks were irradiated with 44.5±0.2 MeV protons at JULIC at FZJ; one stack irradiated for 60 min with beam current of 200 nA and the other irradiation for 26 min while beam current was 115 nA. The details of sample preparation, irradiation and proton beam intensity determination have been reported elsewhere [15,16]. The 88-Inch Cyclotron at LBNL of USA and FZJ allowed Uddin during his short visit to irradiate additional foils of Al, Ti, Fe and Cu together with original experiment of Sr target. Radioactivities of product radionuclides were measured at LBNL and FZJ, respectively, and all the analysis was performed in Bangladesh.

The computer program, STACK, written at FZJ and based on the energy-range relation [17], was utilized to determine the beam energy degradation along the stack.

2.2 Radioactivity measurement and analysis

The activities of the radionuclides formed in titanium target samples were measured by using a HPGe γ-ray detector associated with the necessary electronics and Maestro data acquisition software. The HPGe γ-ray spectroscopy facilities at FZJ, Germany, and LBNL, USA were utilized to measure radioactivity of reaction products. The energy resolutions (FWHM) at 1332.5 keV of ^{60}Co of the HPGe detectors used were 1.9 keV at FZJ and 2.5 keV at LBNL. The efficiency vs energy curve of the detector was determined using the standard point sources ^{54}Mn, ^{133}Ba, ^{137}Cs and ^{152}Eu (supplied by Isotope Products Laboratories) at LBNL, and at FZJ ^{22}Na, ^{54}Mn, ^{57}Co, ^{60}Co, ^{88}Y, ^{137}Cs, ^{152}Eu, ^{226}Ra and ^{241}Am, supplied by Eckert & Ziegler, Berlin. The uncertainty in the activity of each source was specified as 3 %. The γ-ray spectra measured in this work were analyzed by both the GammaVision and FitzPeaks [18] software. The counting was done repeatedly in several time segments depending on the half-life of the radionuclide. Measurements were carried out at a distance of 10 cm, 20 cm and 30 cm from the surface of the detector to keep the detector dead time below 5%. At these counting positions, the effect of extended sample-size on the efficiency, and the random and true coincidence losses were negligible. The decay data of the investigated radionuclides were taken from some recent references [19-22] compiled in ENSDF; they are collectively given in Table 1.

Table I Decay data of the product radionuclides

Radionuclide	Spin/ Parity	Decay Mode (%)	Half life	E_γ (keV)	I_γ (%)	Contributing reactions	Q-value (MeV)
^{48}V	4+	EC=100	15.974 (3) d	983.53 1312.11	99.98(4) 98.2 (3)	^{47}Ti(p,γ) ^{48}Ti(p,n) ^{49}Ti(p,2n) ^{50}Ti(p,3n)	6.83 -4.80 -12.94 -23.88
^{43}Sc	7/2 $^-$	EC=100	3.891 (12) h	372.9	22.5	^{46}Ti(p,α) ^{47}Ti(p,nα) ^{48}Ti(p,2nα) ^{49}Ti(p,3nα)	-3.08 -11.96 -23.58 -31.73
^{44m}Sc	6+	IT=98.77 EC=1.23	58.61 (10) h	271.25	87.8	^{46}Ti(p,n2p) ^{47}Ti(p,α) ^{48}Ti(p,nα) ^{49}Ti(p,2nα) ^{50}Ti(p,3nα)	-14.22 -2.53 -14.54 -22.29 -33.24
^{44g}Sc	2+	EC=100	4.0420 (25) h	1157.02	99.8867(30)	^{46}Ti(p,n2p) ^{47}Ti(p,α) ^{48}Ti(p,nα) ^{49}Ti(p,2nα) ^{50}Ti(p,3nα)	-13.94 -2.26 -13.88 -22.03 -32.96
^{46}Sc	4+	β^-=100	83.79 (4) d	889.28 1120.55	99.984 (1) 99.987 (1)	^{47}Ti(p,2p) ^{48}Ti(p,^{3}He) ^{49}Ti(p,α) ^{50}Ti(p,nα)	-10.47 -14.37 -1.94 -12.88
^{47}Sc	7/2 $^-$	β^-=100	3.3492 (6) d	159.38	68.3 (4)	^{48}Ti(p,2p) ^{49}Ti(p,^{3}He) ^{50}Ti(p,α)	-11.45 -11.87 -2.23
^{48}Sc	6+	β^-=100	43.71 (9) h	175.36 1037.52	7.47(18) 97.5 (20)	^{49}Ti(p,2p) ^{50}Ti(p,^{3}He)	-11.35 -14.57

The radioactivity of the short-lived products, namely ^{43}Sc ($T_{1/2}$=3.891 h) and ^{44g}Sc ($T_{1/2}$=4.042 h) was measured within 6 -12 h after the end of bombardment (EOB). Due to the weak peak and low intensity, peak at 372.76 keV for ^{43}Sc was not appeared in the spectrum of a few titanium target. Thereafter, about 30 h after EOB was allowed to suppress the background and undesired short-lived radionuclides, and comparatively long-lived products were measured for several hours to obtain good counting statistics.

The ground state ^{44g}Sc ($T_{1/2}$=4.042 h) is formed via direct interactions of protons with natural titanium. Its also produced by isomeric transition of the metastable state ^{44m}Sc ($T_{1/2}$=58.61 h). A clear peak at energy of 1157.0 keV emitted in the decay of ^{44g}Sc was appeared in the spectrum. The radionuclide ^{44m}Sc was characterized with a clear peak at 271.241 keV in the spectrum. The total activity of 1157.0 keV gamma-ray energy resulted from the decay of the directly and indirectly-produced ^{44g}Sc radioactivities. Due to the long half-life of ^{44m}Sc, the daughter ^{44g}Sc activity grows to a maximum and then decreases at a constant rate which depends on the decay rate of the parent ^{44m}Sc [23,24], i.e., to reach the parent–daughter transient equilibrium, ^{44m}Sc – ^{44g}Sc. Therefore, the specific counts under the peak at 1157.0 keV for ^{44g}Sc formed via IT of ^{44m}Sc could be estimated from the counts of the peak 271.24 keV, the intensity and detector efficiency of the two radionuclides by considering half-life of the parent in both cases. This value was subtracted from total counts under the 1157.0 keV peak and obtained the counts for the direct production of ^{44g}Sc.

The beam current of each irradiation was measured by charge integration, which provided only an approximate value. As described in [15,16], the proton flux effective in the samples was also determined by activation of Cu and Ti monitors placed in front of a stack. From the measured ^{48}V and ^{62,63,65}Zn activities formed in the Cu and Ti targets, respectively and the IAEA recommended cross sections of the monitor reactions ^{nat}Cu(p,x)^{62,63,65}Zn and ^{nat}Ti(p,x)^{48}V [25], effective proton flux was determined and considered constant along the stack.

The count rate of each product radionuclide was extrapolated to the end of bombardment (EOB) and thereafter converted to decay rate by introducing the necessary corrections for the efficiency of the detector and the intensity of the γ-ray. From the decay rate at EOB and the measured proton beam flux, the cross section for the formation of the radioactive product was calculated using the well-known activation equations. The uncertainty in the measured cross section value was determined from the uncertainties associated with measurements: peak area (0.2-8%), efficiency of the detector (4%), γ-ray intensities (0.0001-1.2%), half-life (0.02-0.3%) and proton flux (6 %). The overall uncertainty of measured cross sections amounted to 7-14% (1σ). Due to weak unsmooth peak at 372.76 keV emitted in the decay of ^{43}Sc, a large uncertainty was associated in the peak area analysis particularly in lower energy region (<16 MeV) as well as with its measured cross section.

3. Nuclear model calculation

Theoretical calculations for the cross sections of radionuclide production resulting from proton-titanium interactions were conducted using the TALYS-1.95 code [26], developed by Koning et al. [27]. This sophisticated code integrates various nuclear models to evaluate all significant nuclear reaction mechanisms over an energy range from 1 keV to 200 MeV. It incorporates typical precompound and compound nucleus processes to calculate cross sections for products formed in proton-induced reactions on titanium. Generally, the results obtained using a global set of parameters from the TENDL file [28] are inadequate for accurately predicting experimental outcomes. Consequently, special emphasis was placed on the careful selection of input parameters to better reproduce the experimental data.

Some of the free parameters in the nuclear reaction models include optical model potential, level density formalism, spin distribution of the level density, and the γ-ray strength function. The values of the input parameter Pshiftadjust (adjustable pairing shift for adjustment of the Fermi Gas level density) were set to -0.1, -0.1, 1.5 and 0.25 were chosen for the ^{43}Sc, ^{44}Sc, ^{47}Sc and ^{48}Sc radionuclides, respectively. These values fall within the recommended limits [28]. The energy, spin, parity, and branching ratios for discrete levels were based on the RIPL-3 database [29]. The spin distribution of the level density was characterized by the ratio of the effective moment of inertia to the rigid-body moment of inertia ($\eta = \Theta_{eff}/\Theta_{rigid}$). For the best fitting of our ^{43}Sc data η=0.98 was used; for ^{44}Sc, η=0.98; for ^{47}Sc, η=0.85; and for ^{48}Sc, η=0.80. Those values were obtained from the systematics based on the evaluation by Sudár and Qaim [30].

4. Results and discussion

Table II provides the measured cross sections for the $^{nat}Ti(p,x)$ reactions, covering energy ranges from reaction thresholds up to 44.28 MeV, along with their associated uncertainties. At the Lawrence Berkeley National Laboratory (LBNL), data were measured from 15 to 25 MeV, while at Forschungszentrum Jülich (FZJ), measurements were taken in the energy ranges of 14-44.28 MeV and 8-16.21 MeV. These data are shown as a function of proton energy in Figures 1 to 7.

Table II Measured cross sections with uncertainty for the investigated product radionuclides.

Proton energy (Mev)	Cyclotron	Cross section (mb)				
		^{43}Sc	^{44m}Sc	^{44g}Sc	^{47}Sc	^{48}Sc
44.28	JULIC	16.93±1.50	12.62±0.88	26.00±2.35	17.63±1.57	1.59±0.143
43.54			12.47±0.91		17.25±1.55	1.54±0.14
41.99			13.67±1.01		17.04±1.53	1.38±0.15
39.63			14.45±1.07		17.37±1.56	1.27±0.13
39.20		10.59+0.94	13.33±0.99	24.58±2.16		1.11±0.099
37.14			16.32±1.24		18.37±1.65	1.15±0.12
34.14			17.11±1.25		19.74±1.78	0.95±0.11
31.38			17.57±1.29		21.18±1.91	0.71±0.08
29.94		2.65±0.25	14.84±1.10	44.87±3.95	20.34±1.84	0.60±0.054
29.23			15.77±1.16		19.47±1.75	0.58±0.06
23.89		2.95±0.28	6.81±0.53	23.41±2.06	11.43±1.01	0.23±0.058
22.63			3.88±0.28			0.18±0.02
19.16		2.67±0.25	1.11±0.14	2.69±0.24	3.80±0.37	0.10±0.011
18.04		3.44±0.32	1.18±0.19	3.88±0.34	3.22±0.35	0.03±0.007
15.93		3.33±0.30	1.10±0.15	3.66±0.32	1.36±0.17	
14.70		3.45±0.31	0.81±0.13	4.29±0.38	1.16±0.17	
24.91	88-Inch	2.88±0.27	7.88±0.57	24.49±2.15	12.43±1.09	
23.40		2.77±0.26	5.28±0.38	15.50±1.36	10.98±0.97	
21.41		2.56±0.24	2.14±0.16	4.99±0.44	8.06±0.71	
19.34		2.70±0.28	1.13±0.08	2.51±0.22	5.07±0.45	
16.57		3.41±0.41	1.09±0.08	3.66±0.33	1.83±0.16	
15.36		3.59±0.52	0.98±0.07	3.76±0.34	1.16±0.10	
16.21	BC1710	3.71±0.34				
15.97		3.61±0.69	1.22±0.122	4.24±0.55	1.58±0.15	
15.59			1.10±0.110		1.13±0.11	
14.73		3.49±0.74	0.93±0.093	4.12±0.64	1.16±0.12	
13.44		3.05±0.95	0.72±0.072	3.75±0.62	0.73±0.08	
12.03			0.41±0.045	2.87±0.79	0.58±0.08	
10.51		1.48±0.39	0.26±0.061	1.82±0.55	0.41±0.05	
9.66		1.19±0.12			0.29±0.04	
8.77			0.10±0.023	0.79±0.24	0.21±0.03	
8.73			0.03±0.008			

4.1 ^{nat}Ti(p,x)^{48}V and ^{nat}Ti(p,x)^{46}Sc reactions: Validation of experimental techniques

We measured the excitation function of the ^{nat}Ti(p,x)^{48}V and ^{nat}Ti(p,x)^{46}Sc reactions in all experiments to validate our experimental techniques. The measured values from the experiments performed agreed well in the overlapping region. We chose these reactions because the International Atomic Energy Agency (IAEA) has provided recommended data for them after critically evaluating numerous data sets from various groups worldwide [25]. Comparing our experimental values with the recommended ones allows us to assess the degree of agreement or deviation. The data obtained in this study and the IAEA-recommended values are presented in Figs. 1 and 2. The agreement between our data and the recommended curve across the entire investigated energy range is excellent, providing high confidence in our measurements. This agreement demonstrates the reliability of the various techniques used in this work at LBNL and FZJ, particularly the efficiency determination of the γ-ray counting system, and the energy and intensity measurement of the proton beam.

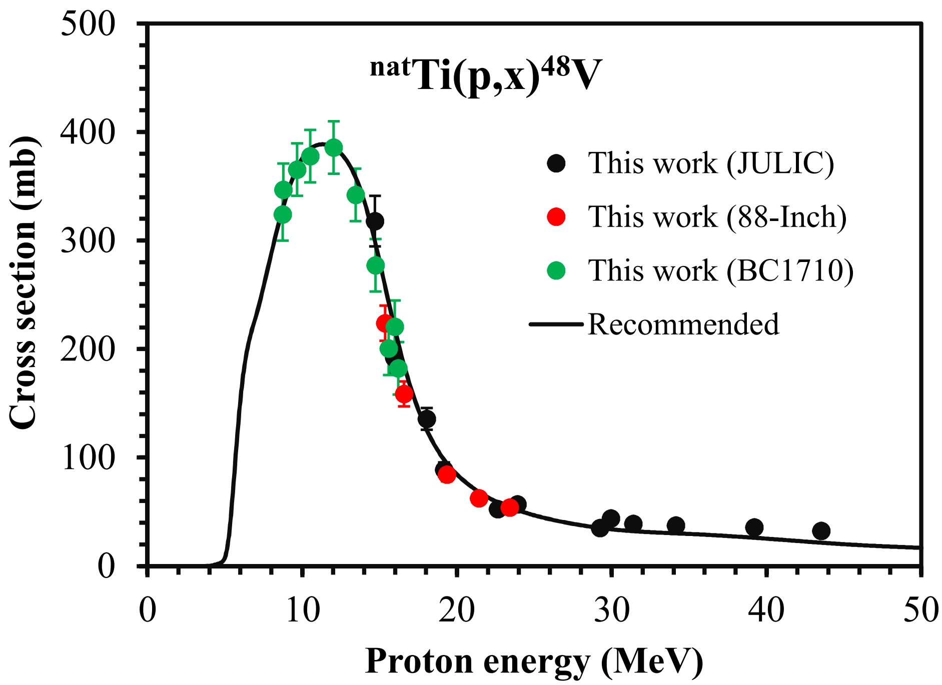

Fig. 1 Comparison of the measured data of ^{nat}Ti(p,x)^{48}V with the IAEA recommended curve.

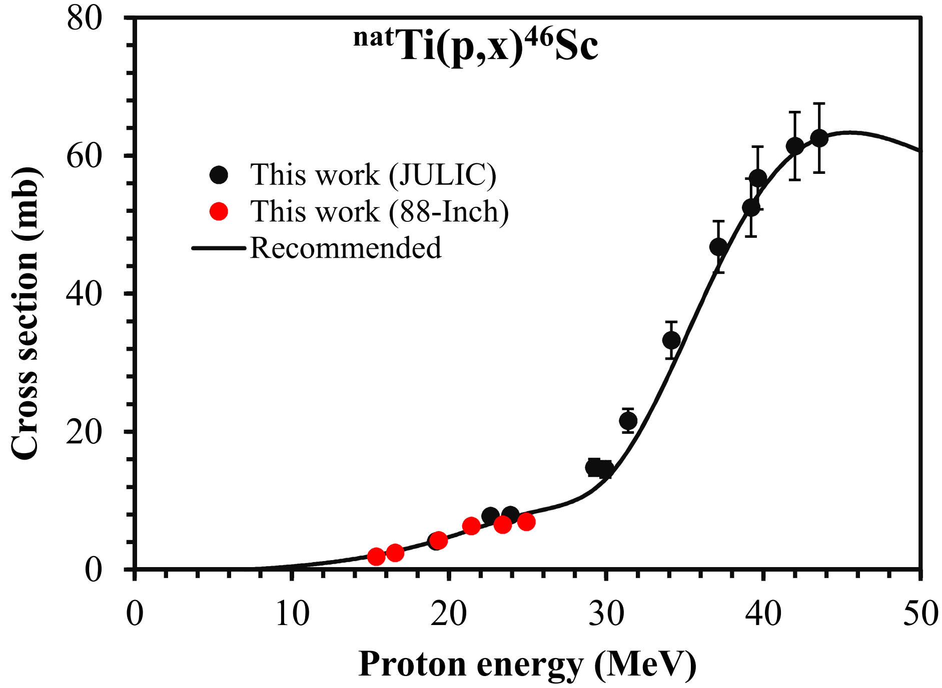

Fig. 2 Comparison of the measured data of $^{nat}Ti(p,x)^{46}Sc$ with the IAEA recommended curve.

4.2 $^{nat}Ti(p,x)^{43}Sc$

The measured cross sections for the production of ^{43}Sc in interactions of protons with the titanium of natural isotopic composition are depicted in Fig.3 together with results of model calculations using the TALYS code. The radionuclide ^{43}Sc was formed via two reactions $^{46}Ti(p,\alpha)^{43}Sc$ (E_{th}= 3.14 MeV) and $^{47}Ti(p,n\alpha)^{43}Sc$ (E_{th}= 12.21 MeV) from the reaction threshold to 30 MeV. The model calculations using TALYS code reproduced well our measured data.

The detailed model calculations, i.e. the results of the individual processes are shown in Fig. 3 after convertion to natural titanium target. The excitation function for ^{43}Sc exhibits a peak at around 16 MeV, a valley from 19 to 30 MeV, and beyond this energy sharply raising, and these confirm various reactions contributing to the ^{43}Sc production with the proton energy changes. The first peak at 15 MeV is only due to the $^{46}Ti(p,\alpha)^{43}Sc$ reaction. In the broad valley from 19 to 30 MeV, the $^{47}Ti(p,n\alpha)^{43}Sc$ reaction dominates the formation of ^{43}Sc. Noted that α particle showing a single particle character, here multi nucleon emission has not occurred.

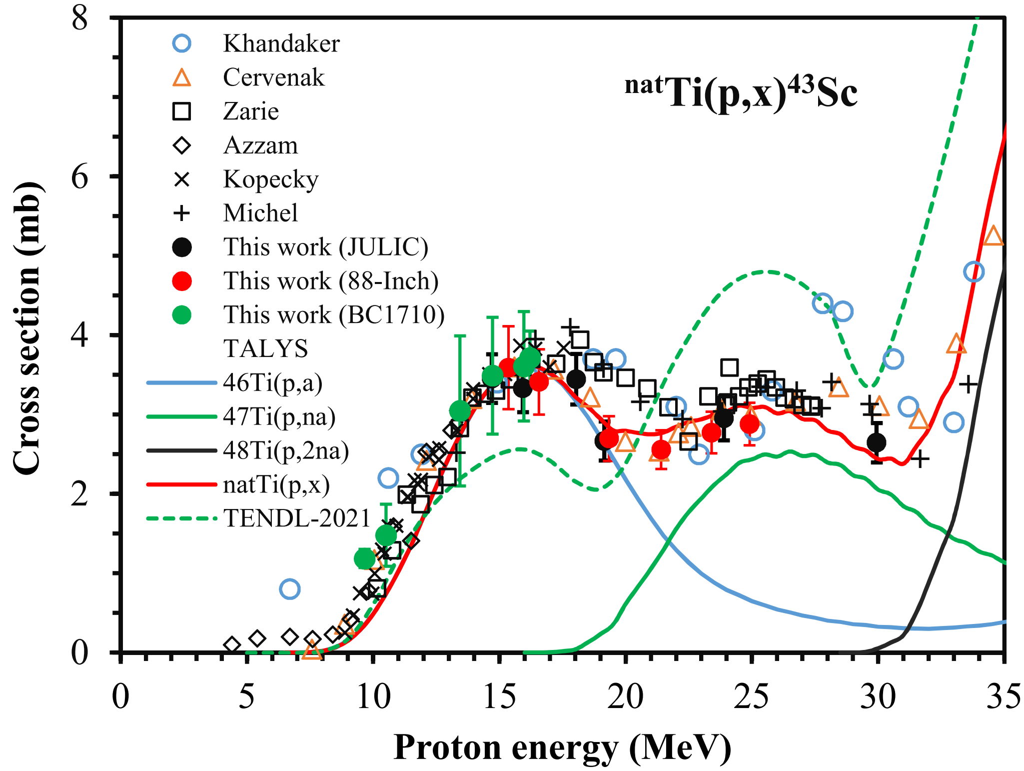

Fig. 3 Comparison of experimental data with results of model calculations using the TALYS code. This figure showing the individual contributions to the formation of ^{43}Sc in protons on ^{nat}Ti; the results of calculations for the ^{46}Ti(p,α)^{43}Sc and ^{47}Ti(p,nα)^{43}Sc reactions converted to natural titanium target.

4.3 ^{nat}Ti(p,x)^{44m}Sc

The ^{44}Sc radionuclide has two isomeric state; ground state ^{44g}Sc ($T_{1/2}$=4.042 h) and metastable state ^{44m}Sc ($T_{1/2}$=58.61 h). The metastable state decays by 98.77% isomeric transition and 1.23 % EC. The metastable state ^{44m}Sc was formed in the interaction of protons with stable isotopes, ^{46}Ti (8.25%), ^{47}Ti (7.44%), ^{48}Ti (73.72%), ^{49}Ti (5.41%) and ^{50}Ti (5.18%) in natural target. The measured data are the sum of the cross sections of the processes, ^{46}Ti(p,n2p), ^{47}Ti(p,α), ^{48}Ti(p,nα), ^{49}Ti(p,2nα) and ^{50}Ti(p,3nα) depending on their reaction thresholds. In the higher energy region, a significant contribution of multinucleon emission in place of a single α-particle emission is also expected. The measured cross sections for the production of ^{44m}Sc are shown in Fig. 4 together with other experimental data and the results of model calculations using the TALYS code.

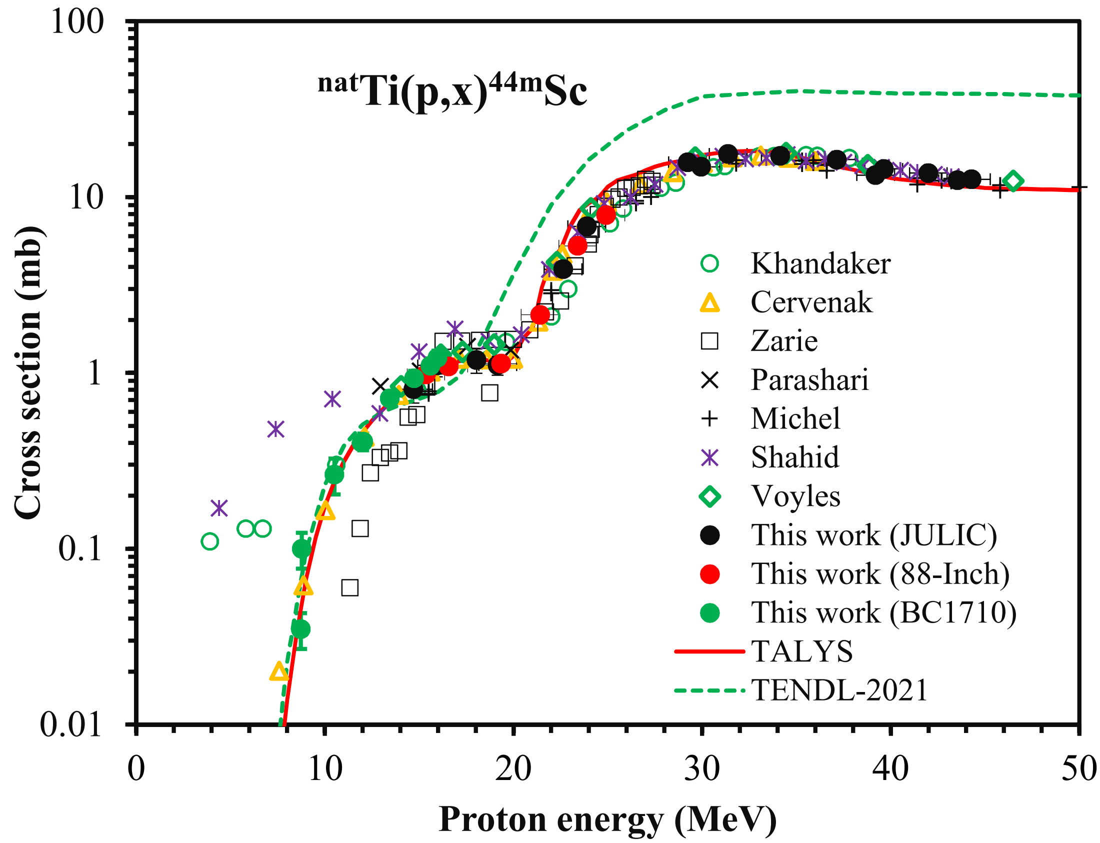

Fig. 4 Comparison of experimental data of $^{nat}Ti(p,x)^{44m}Sc$ with results of model calculations using the TALYS code.

The model calculations reproduced well our measured data both in shape and magnitude. As seen in Fig. 4, the peak at around 18 MeV is due to the $^{47}T(p,\alpha)^{44m}Sc$ reaction, it raises sharply with the increase of energy and reach to the another peak at around 32 MeV where the $^{48}Ti(p,n\alpha)$ reaction pricipally dominated the production of ^{44m}Sc. Beyond this energy many channels open to contribute on the ^{44m}Sc production. The measured values are in good agreement with other reported data accept below 10 MeV. Červenák and Lebeda [5] reported data from 7 to 36 MeV and those values supported well our experimental results as well as model calculations. Bellow 10 MeV the data reported by Khandaker et al.[11] and Shahid et al.[6] are not comparable, and thus deviation can be described by i) a big energy span from 3.9 to 37.8 MeV and 4.4 to 43.2 MeV in a single irradiation, and ii) a large uncertainty associated with the analysis of weak unsmooth peak in the lower energy region. In this work, three sets of experimental data were obtained from irradiations with primary proton beam energyies of 16.7 MeV, 27 MeV and 44.5 MeV and each data set is consistent with others in the overlapping energy region. Similarly Červenák and Lebeda reported data from 7 to 36 MeV obtained from the irradiations of two stacks with proton beam of 21.35 MeV and 36 MeV, and those values supported well our experimental results as well as model calculations. The data of Zarie et al.[8] are seemed to be shifted downward and no reason was found for their unexpected data below 25 MeV.

4.4 $^{nat}Ti(p,x)^{44g}Sc$

The ^{44g}Sc radionuclide was formed in direct interaction of protons with titanium and in IT decay of metastable state ^{44m}Sc. The half-life of ^{44m}Sc ($T_{1/2}$=58.61 h) is long comparing to the ground state ^{44g}Sc ($T_{1/2}$=4.042 h) and its decay to ground state was not homogeneous for all samples because of their different cooling time and counting time. Therefore, the ^{44g}Sc activity with respect to the decay of ^{44m}Sc was subtracted from the total measured activity. Our measured cross-section values are only for the formation of ^{44g}Sc through direct processes. We have three sets of the measured data and each set is consistent with other in the overlapping energy region. The experimental cross sections for the ^{44g}Sc production via the direct proton-induced reactions on natural titanium are depicted in Fig.5 together with results of model calculations using the TALYS code. In interaction of protons in the natural titanium target irradiation, ^{44g}Sc can be formed via many channels and it is difficult to analyse individually all contributing processes. However, the contributions of all posibble processes are included in the measured values, and same was done in calculations. The model calculations reproduced well experimental values. The detailed model calculations, i.e. the results of calculations for the individual processes $^{46}Ti(p,n2p)^{44g}Sc$, $^{47}Ti(p,\alpha)^{44g}Sc$, $^{47}Ti(p,2n2p)^{44g}Sc$, $^{47}Ti(p,npd)^{44g}Sc$, $^{47}Ti(p,n^{3}He)^{44g}Sc$, $^{48}Ti(p,n\alpha)^{44g}Sc$, $^{49}Ti(p,2n\alpha)^{44g}Sc$ and $^{50}Ti(p,3n\alpha)^{44g}Sc$ are shown in Fig. 5 after convertion to natural titanium target.

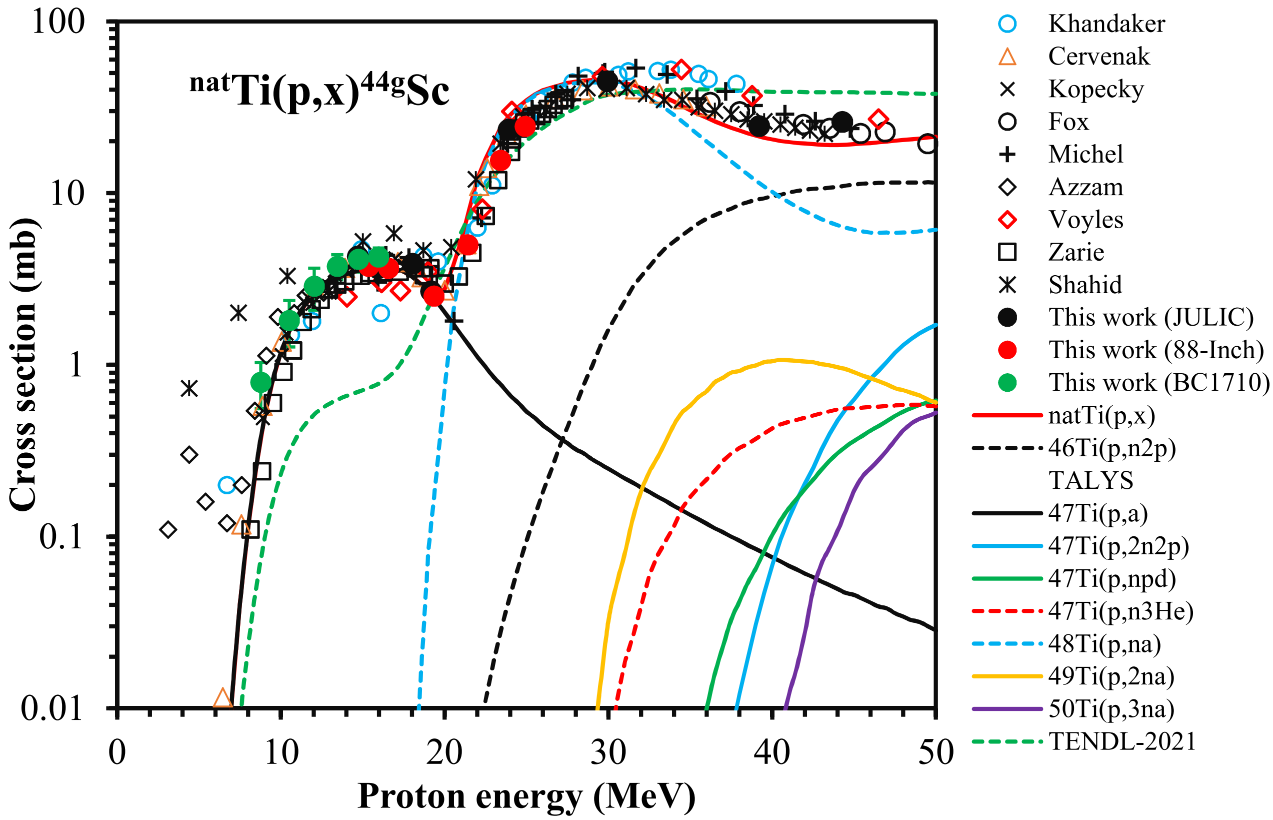

Fig. 5 Comparison of experimental data with results of model calculations using the TALYS code. This figure showing the individual contributions to the formation of ^{44g}Sc in protons on ^{nat}Ti. Detailed results of model calculations using the TALYS code for the ^{nat}Ti(p,x)^{44g}Sc process; the results of calculations for the ^{46}Ti(p,n2p)^{44g}Sc, ^{47}Ti(p,α)^{44g}Sc, ^{47}Ti(p,2n2p)^{44g}Sc, ^{47}Ti(p,npd)^{44g}Sc, ^{47}Ti(p,n^{3}He)^{44g}Sc, ^{48}Ti(p,nα)^{44g}Sc, ^{49}Ti(p,2nα)^{44g}Sc and ^{50}Ti(p,3nα)^{44g}Sc reactions were converted to natural titanium target.

The peak at around 16 MeV is due to sole contribution of the process ^{47}Ti(p,α)^{44g}Sc. As depicted in Fig. 5, from reaction threshold to 20 MeV the radionuclide ^{44g}Sc was formed only by the channel ^{47}Ti(p,α). Above 20 MeV its production cross section sharply rises due to openning a new channel ^{48}Ti(p,nα), reach a maxima at around the second peak at 30 MeV and it dominates up to 39 MeV due to the highest abundance (73.72%) of the ^{48}Ti isotope in natural target. Beyond this energy a sigificant formation of ^{44g}Sc was due to the contribution to multinucleon emission, which is larger compairing to the single particle emission.

Khadaker et al.[11] reported cross sections of the ^{nat}Ti(p,x)^{44g}Sc process from 6.7 to 37.8 MeV. Some reported values are consistent with other experimental data, few values particularly from 28 to 37.8 MeV are significantly higher and this can be described with the incorrect decay data, e.g. half-life 3.93 h used in place of the latest value 4.042 h and the decay of metastable state ^{44m}Sc to the ground state ^{44g}Sc was not corrected and its effect was not homogenous in measurements for all targets. Similar trend was followed by Voyles et al.[12] and Michel et al.[10] from 28 to 40 MeV, where all experimental data are divided into two groups. The data of other groups of Shahid et al.[6], Zarie et al.[8] and Červenák and Lebeda [5] supported our data and model calculations and it confirms that the contribution of the IT decay of ^{44m}Sc was properly subtracted and their data represent the direct processes.

4.5 ^{nat}Ti(p,x)^{47}Sc

The measured cross sections for the production of ^{47}Sc in proton induced activation on natural titanium are shown in Fig. 6. The available other experimental data and the results of model calculations using the code TALYS are also shown in figure. Since natural titanium was used as target, many channels were opened to contribute in production of ^{47}Sc. The measured values include all the possible processes. The individual feeding of those processes was calculated theoretically with the code TALYS and the results of the individual processes ^{48}Ti(p,2p)^{47}Sc, ^{49}Ti(p,n2p)^{47}Sc ^{50}Ti(p,α)^{47}Sc, ^{50}Ti(p,2n2p)^{47}Sc, ^{50}Ti(p,npd)^{47}Sc and ^{50}Ti(p,n^{3}He)^{47}Sc are shown in Fig. 6 after convertion to natural titanium target. Thus helped us to describe the excitation function in detail. The model calculations reproduced well our measured data. As sheen in Fig.6, no clear peak at around 19 MeV for the (p,α) process is appeared in the down stream of the measured excitation function because of the big contribution of the (p,2p) process in the expected peak region. On the other hand in the peak region at around 32 MeV the ^{48}Ti(p,2p) reaction dominated the ^{47}Sc production. Noted that above 40 MeV the contribution of mutlinucleon emission is larger compairing to a single particle emission.

Our measured data are consistent with other reported values within the uncertainty limit. As seen before for other radionuclides, below 7 MeV the data reported by Khandaker et al. Azzam et al. and Shahid et al. are shifted downward and it may be described uncorrect effective proton beam energy because of a large uncertainty added on the lowest energy of big span obtained through stacked activation using the high energy of priliminary incident beam, i.e. Khanader et al. reported data in the energy region of 4–38 MeV via a single irradiation of stacked-foils with proton beam of 42.1 MeV and the similar was found to Azzam et al. and Shahid et al.

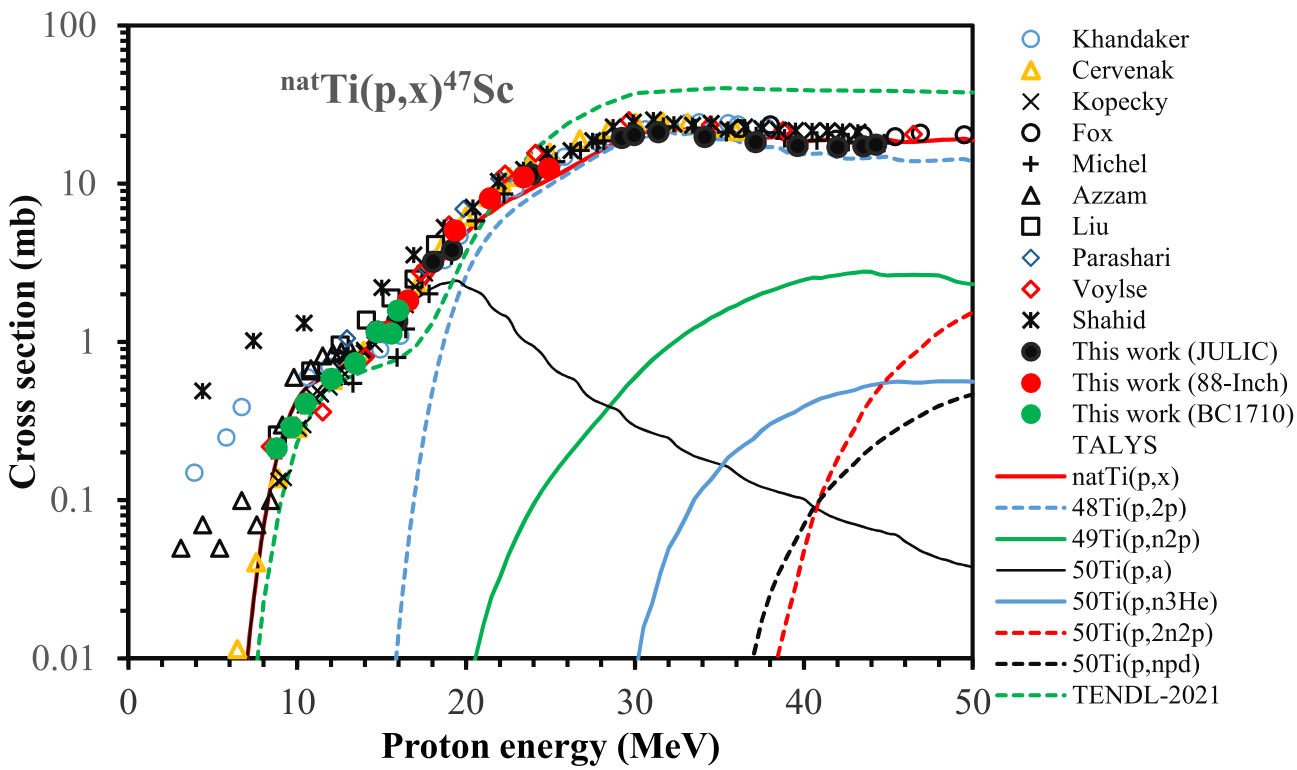

Fig. 6 Comparison of experimental data with results of model calculations using the TALYS code. This figure showing the individual contributions to the formation of ^{47}Sc in protons on ^{nat}Ti. Detailed results of model calculations using the TALYS code for the ^{nat}Ti(p,x)^{47}Sc process; the results of calculations for the ^{48}Ti(p,2p)^{47}Sc, ^{49}Ti(p,n2p)^{47}Sc ^{50}Ti(p,α)^{47}Sc, ^{50}Ti(p,2n2p)^{47}Sc, ^{50}Ti(p,npd)^{47}Sc and ^{50}Ti(p,n^{3}He)^{47}Sc reactions were converted to natural titanium target.

4.6 ^{nat}Ti(p,x)^{48}Sc

The study presents measured cross sections for the formation of ^{48}Sc through the interaction of protons with ^{49}Ti and ^{50}Ti in natural titanium. These measurements are displayed in Fig. 7 alongside other experimental data and model calculations. The cross sections were determined from the peak areas of two gamma rays, at 175.36 keV and 1037.52 keV, emitted during the decay of ^{48}Sc. The average of the two individual values for each sample was calculated. The measured data show an increase with rising proton energy within the investigated energy range. The results of this study are consisntent with previously reported experimental data within the uncertainty limits. The model calculations accurately reproduced the experimental data in both shape and magnitude.

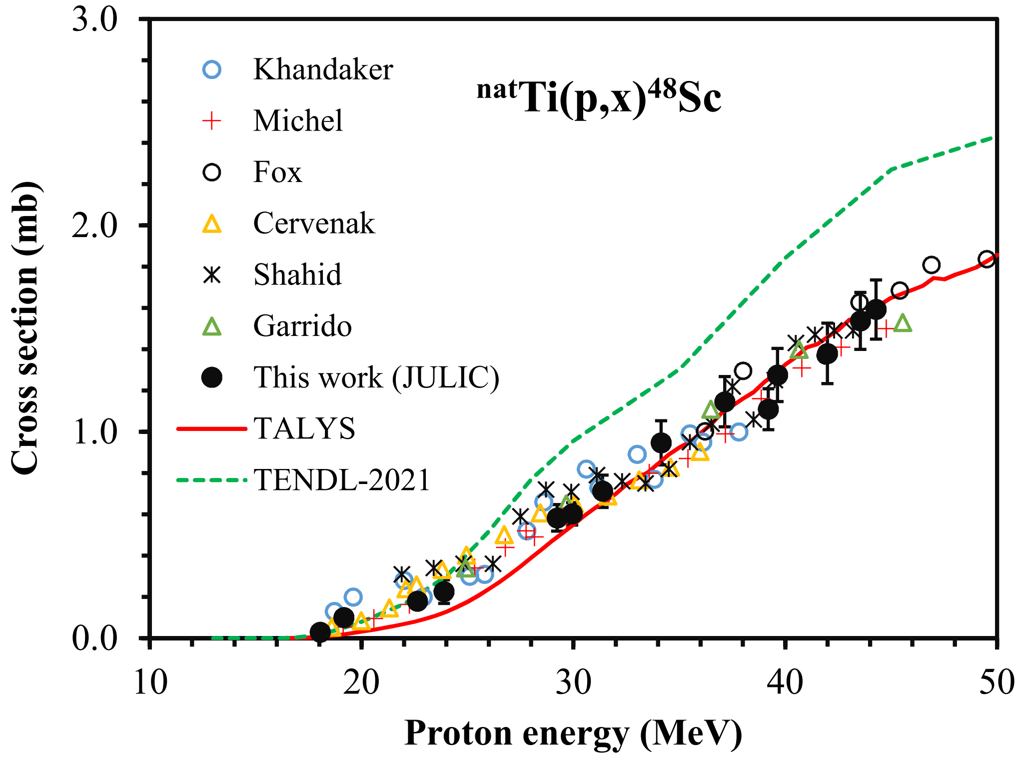

Fig. 7 Comparison of experimental data of $^{nat}Ti(p,x)^{48}Sc$ with results of model calculations using the TALYS code.

5. Conclusion

In this study, we have successfully obtained new cross-section data for the $^{nat}Ti(p,x)^{43,44m,44g,47,48}Sc$ reactions from their respective thresholds up to 44.28 MeV using natural titanium targets. The experimental results were found to align well with theoretical predictions made by the TALYS code after the proper choice of input parameters. This alignment confirms the accuracy and reliability of our data, effectively addressing and resolving the discrepancies present in previous datasets. Consequently, the nuclear data library for proton-induced reactions on titanium has been significantly strengthened, extending its coverage up to 44.28 MeV.

The study employed proton beam irradiations at multiple energies 16.5 MeV, 27 MeV, and 44.5 MeV, enabling us to achieve precise cross-section data in the ranges of 15 to 25 MeV at LBNL, and 14 to 44.28 MeV and 8 to 17 MeV at FZJ. This approach has also helped in reducing uncertainties, particularly for the lower energy of stack measurements. Our data demonstrates excellent agreement in overlapping energy regions, further validating the quality of our findings.

Typically, results derived from the use of a global set of parameters, as outlined in the TENDL file, are inadequate for accurately predicting experimental outcomes. However, better match of the experimental data with the model calculations using the TALYS code after carefully selected specific input parameters.

These new measurements provide valuable contributions not only for resolving existing data inconsistencies but also for optimizing the production of medical isotopes and offering insights into reaction mechanisms. The enhanced database can serve as a reliable reference for future research and practical applications in nuclear medicine and industry.

References

1. Qaim S.M., Scholten B., Neumaier B. New developments in the production of theranostic pairs of radionuclides. *J. Radioanal. Nucl. Chem.* **2018,** 318,1493-1509.
2. Uddin, M.S., Chakraborty, A.K., Spellerberg, S., Shariff, M.A., Das, S., Rashid, M.A., Spahn, I., Qaim, S.M. Experimental determination of proton induced reaction cross sections on ^{nat}Ni near threshold energy. *Radiochim. Acta*. **2016**,104, 305.
3. Liu B., Han R., Yuan C., Sun H., Chen Z., Tian G., Shi F., Zhang X., Luo P., Jia H.:Excitation functions of proton induced reactions on titanium and copper. *Appl. Radiat. Isot.* **2021**, 173, 109
4. Azzam A., Hamada M.S., Said S.A., Mohamed G.Y., Al-abyad M. Excitation functions for proton-induced reactions on Te and ^{nat}Ti targets: Measurements and model calculations special relevant to the ^{128}Te(p,n)^{128}I reaction. *Nucl. Phys. A* **2020**, 999, 121790.
5. Červenák J., Lebeda O. New cross-section data for proton-induced reactions on ^{nat}Ti and ^{nat}Cu with special regard to the beam monitoring. *Nucl. Instrum. Method. Phys. Res. B* **2020**, 480, 78-97.
6. Shahid M., Kim K., Kim G.N., Naik H.: Measurement of excitation functions of residual radionuclides from ^{nat}Ti(p,x) reactions up to 44 MeV. J. Radioanal. Nucl. Chem. **318**, 2049 (2018).
7. Garrido E., Duchemin C., Guertin A., Haddad F., Michel N., Metivier V. New excitation functions for proton induced reactions on natural titanium, nickel and copper up to 70 MeV. *Nucl. Instrum. Method. Phys. Res. B*, **2016**, 383, 191-212.
8. Zarie K., Al-Hammad N., Azzam A. Experimental study of excitation functions of some proton induced reactions on ^{nat}Ti for beam monitoring purpose. *Radiochim. Acta*. **2006**, 94, 795-799.

9. Kopecky P., Szelecsényi F., Molnár T., Mikecz P., Tárkányi F. Excitation functions of (p,xn) reactions on ^{nat}Ti: monitoring of bombarding proton beams. *Appl. Radiat. Isot.* **1993**, 44, 687-692.

10. Michel R., Brinkmann G., Weigel H., Herr W. Proton-induced reactions on titanium with energies between 13 and 45 MeV. *J. Inorg. Nucl. Chem*. **1978,** 40, 1845.

11. Khandaker M.U., Kim K., Lee M.W., Kim K.S., Kim G.N., Cho Y.S., Lee Y.O. Investigations of the $^{nat}Ti(p,x)^{43,44m,44g,46,47,48}Sc$, ^{48}V nuclear processes up to 40 MeV. *Appl. Radiat. Isot*. **2009**, 67, 1348-1354.

12. Voyles A.S., Lewis A.M., Morrell J.T., Basunia M.S., Bernstein L.A., Engle J.W., Graves S.A., Matthews E.F. Proton-induced reactions on Fe, Cu, and Ti from threshold to 55 MeV. *Eur. Phys. J. A* **2021**, 57, 94.

13. Parashari S., Mukherjee S., Nayak B.K., Naik H., Suryanarayana S.V., Makwana R., Singh N.L. Excitation function of the $^{nat}Ti(p,x)^{48}V$,$^{47,46,44m}Sc$ reactions within the energy range of 10-22 MeV. Nucl. Phys. A **2019**, 987, 128.

14. Fox M.B., Voyles A.S., A.M., Morrell J.T., Bernstein L.A., Batchelder J.C., Birnbaum E.R., Cutler C.S., Koning A.J., Lewis A.M., Medvedev D.G., Nortier F.M., O`Brien E.M., Vermeulen Ch. Measurement and modeling of proton-induced reactions on arsenic from 35 to 200 MeV. *Phys. Rev.C* **2021**, 104, 064615.

15. Uddin M.S**.**, Scholten B**.,** Basunia M.S., Sudár S., Spellerberg S.,, Voyles A.S., Morrell J. T., Zaneb H., Rios J.A., Spahn I., Bernstein L.A., Qaim S.M., Neumaier B. Accurate determination of production data of the non-standard positron emitter ^{86}Y via the. $^{86}Sr(p,n)$-reaction. *Radiochim. Acta*. **2020**. 108, 747-756.

16. Uddin M.S., Basunia M.S., Sudár S., Scholten B., Spellerberg S., Voyles A.S., Morrell J.T., Fox M.B., Spahn I., Felden O., Gebel R., Bernstein L.A., Neumaier B., Qaim S.M. Excitation functions of proton-induced nuclear reactions on ^{86}Sr, with particular emphasis on the formation of isomeric states in ^{86}Y and ^{85}Y. *European Phys. Jour.* A **2022**, 58: 67**.**

17. Williamson C.F., Boujot J.P., Picard J. Tables of range and stopping power of chemical elements for charged particles of energies from 0.5 to 500 MeV. Report CEA-R 3042 (1966).

18. Fitzgerald J. JF Computing Services, 17 Chapel Road, Stanford in the Vale, Oxfordshire, SN7 8LE. Copyright © Jim Fitzgerald 1991-2016, Last updated 8th October 2016.

19. Singh B. Chen J. Nuclear Data Sheets for A=43. *Nucl. Data Sheets* **2015**, 126, 1-150.

20. Chen J., Singh B. Nuclear Structure and Decay Data for A=44 Isobars. *Nucl. Data Sheets* **2023**, 190, 1-318.

21. Burrows T.W. Nuclear Data Sheets *for A = 47*. *Nucl. Data Sheets* **2007**, 108, 923-1056.

22. Chen . Nuclear Data Sheets *for A=48. Nucl. Data Sheets* **2022**, 179, 1-382.

23. Uddin M.S., Hagiwara M., Tárkányi F., Ditrói F., Baba M. Experimental studies on the proton-induced activation reactions of molybdenum in the energy range 22-67 MeV. *Appl. Radiat. Isot*. **2004**, 60, 911-920.

24. Uddin M.S., Afroze N., Hossain S.M., Zakaria A.K.M., Islam M.A., Azharul Islam S.M. Measurement of cross section of the $^{98}Mo(n,\gamma)^{99}Mo$ reaction using monochromatic thermal neutrons. *Radiochim. Acta* **2015,** 103(2), 85-90.

25. Hermanne A., Ignatyuk A.V., Capote R., Carlson B.V., Engle J.W., Kellett M.A., Kib´edi T., Kim G., Kondev F.G., Hussain M., Lebeda O., Luca A., Nagai Y., Naik H., Nichols A. L., Nortier F.M., Suryanarayana S.V., Takács S., Tárkányi F., Verpelli M.Reference cross sections for charged-particle monitor reactions. *Nucl. Data Sheets* **2018**, 148, 338-382.

26. Koning A., Hilaire S., Goriely S. TALYS: modeling of nuclear reactions. *Eur. Phys. J. A* **2023**, 59**,** 131.

27. Koning A.J., Hilaire S., Duijvestijn M.C. TALYS-1.0. Proc .International Conference on Nuclear Data for Science and Technology, April 22-27, 2007, Nice, France, editors: Bersillon O., Gunsing F., Bauge E., Jacqmin R., Leray S. EDP Sciences, 2008, pp. 211-214.

28. Koning A.J., Rochman D., van der Marck S.C., Kopecky J., Sublet J. Ch., Pomp S., Sjostrand H., Forrest R., Bauge E., Henriksson H., Cabellos O., Goriely S. Leppanen I., Leeb H., Plompen A., Mills R. TENDL-2021: TALYS-based evaluated nuclear data library. 30 December 2021.

29. Capote R., Herman M., Oblozinsky P., Young P., Goriely S., Belgya T., Ignatyuk A., Koning A.J., Hilaire S., Plujko V., Avrigeanu M., Chadwick O.B.M., Fukahori T., Kailas S., Kopecky J., Maslov V., Reffo G., Sin M., Soukhovitskii E., Talou P., Yinlu H., Zhigang G. RIPL 3 Reference Input Parameter Library for Calculation of Nuclear Reactions and Nuclear Data Evaluations. *Nucl. Data Sheets* **2009**, 110, 3107.

30. Sudár S., Qaim, S.M. Mass number and excitation energy dependence of the $\Theta_{eff}/\Theta_{rig}$ parameter of the spin cut-off factor in the formation of an isomeric pair. *Nucl. Phys. A* **2018**, 979, 113-142.